Virginia Commonwealth University
VCU Scholars Compass

Theses and Dissertations | Graduate School

2020

Ceramide Synthase 2 Interacts with Ceramide Synthases 5 and 6 at the mRNA and Protein Levels

Dorothy Yen
Virginia Commonwealth University

Follow this and additional works at: https://scholarscompass.vcu.edu/etd

© The Author

Downloaded from
https://scholarscompass.vcu.edu/etd/6407

This Thesis is brought to you for free and open access by the Graduate School at VCU Scholars Compass. It has been accepted for inclusion in Theses and Dissertations by an authorized administrator of VCU Scholars Compass. For more information, please contact libcompass@vcu.edu.

© Dorothy L Yen, 2020

All Rights Reserved

CERAMIDE SYNTHASE 2 INTERACTS WITH CERAMIDE SYNTHASES 5 AND 6 AT mRNA AND PROTEIN LEVELS IN AC16 CELLS

A thesis submitted in partial fulfillment of the requirements for the degree of Masters of Biochemistry at Virginia Commonwealth University.

by

DOROTHY YEN
Bachelor of Arts, Virginia Commonwealth University, 2016
Bachelor of Science, Virginia Commonwealth University, 2016

Director: L. ASHLEY COWART, PhD
PROFESSOR, DEPARTMENT OF BIOCHEMISTRY AND MOLECULAR BIOLOGY

Virginia Commonwealth University
Richmond, Virginia
July 2020

Acknowledgement

I would like to thank my advisor, Dr. L. Ashley Cowart, as well as the members of my committee, Dr. Brian Wattenberg and Dr. Edward Lesnefsky. I would especially like to thank Ashley as well as Dr. William Hancock for bringing me into the this lab and giving me the guidance and resources I needed in order to grow as a scientist and a student. I would also like to thank all the current and former members of the Cowart lab at VCU for being patient with me and my endless questions, as I could not have gotten through this program without them. I would like to thank my parents, Dewey and Mai, for their support over the years. I would also like to extend a big thank you to my roommate, Virali Bhagat, for listening to me whine and complain throughout this whole process.

Table of Contents

Page

List of Figures

Page

Abstract

CERAMIDE SYNTHASE 2 INTERACTS WITH CERS5 AND 6 AT mRNA AND PROTEIN LEVELS IN AC16 CELLS

By Dorothy Yen

A thesis submitted in partial fulfillment of the requirements for the degree of Masters of Biochemistry at Virginia Commonwealth University.

Virginia Commonwealth University, 2020

Major Director: L. Ashley Cowart, PhD
Professor, Department of Biochemistry and Molecular Biology

Ceramides and sphingolipids make up major portions of the plasma membrane and therefore are crucial for cell proliferation, survival, and death. With dysregulation comes numerous pathophysiological conditions, such as Alzheimer's, Huntington's Disease, Creutzfeldt-Jakob, cardiovascular disease, and many cancers. However, the regulation of the enzymes responsible for catalyzing the formation of ceramides is still not well understood. In this experiment, three isoforms were of focus: CerS2, CerS5, and CerS6. Through mRNA, protein, and immunofluorescence analysis, it can be concluded that these isoforms do indeed interact within the human cell in order to upregulate their activity. It was also found that cells made to overexpress CerS2 also tend to express CerS5 and CerS6 to the point of interaction between the two proteins.

CHAPTER 1

Introduction

Sphingolipid metabolism

Sphingolipids are critical regulators of cell growth and differentiation and their dysregulation has been shown to induce stress responses that will eventually lead to various diseases, including Alzheimer's, Huntington's, cardiovascular disease, and human cancers. This class of lipid molecules, which contains a sphingosine backbone, make up a crucial portion of eukaryotic plasma membranes by defining the physical aspect of said membrane. They are heavily engaged at various levels of biological functions and have been thought of as being capable of producing second messenger metabolites as well as acting as second messengers themselves (Zheng et al., 2006).

Sphingolipids can have a variety of fatty acid chain lengths and it has been postulated that those lengths will have a downstream effect on pro-apoptotic or pro-survival signaling. The sphingoid backbone is typically O-linked to a charged head group (which typically determines the molecule's nomenclature) and amide-linked to an acyl group. In humans, the primary sphingolipids are sphingosine (d18:1), sphinganine (d18:0), and 4-hydroxysphinganine (t18:0), though sphingolipid composition has been observed to

rapidly change and therefore alter membrane structure in response to stimulus (Zheng et al., 2006). *De novo* sphingolipid synthesis begins with the condensation reaction between serine and a fatty acyl-CoA (typically palmitoyl-CoA) to form 3-ketosphinganine via serine palmitoyltransferase. 3KSa is reduced to sphinganine via 3-ketosphinganine reductase, N-acylated to dihydroceramide, and desaturated to ceramide, all within the endoplasmic reticulum.

Sphingosine is a long-chain (at 18 carbons), unsaturated amino alcohol that is an essential component to sphingolipids. Ceramide degradation via ceramidase hydrolysis has been considered to be the only source of intracellular sphingosine as there is not yet a direct reaction that can add the appropriate 4,5-double bond to sphinganine (Zheng et al., 2006). The balance between sphingolipids and ceramides is crucial to the body, not only as building blocks and metabolites of one another, but also to maintain a homeostatic balance between pro- and anti-apoptotic molecules. Specifically, ceramides and sphingosine 1-phosphate (S1P), a signaling sphingolipid that also acts as a bioactive mediator, constitute a rheostat system in which they maintain balance between cell death via ceramide production or cell survival via S1P (Lavieu et al., 2007). S1P is formed from ceramide via ceramidase, as was mentioned previously regarding the only known reaction to form sphingosine, and then is phosphorylated via one of two sphingosine kinase isoforms. S1P did not hold significance to this project in particular, but is of importance to discuss when illustrating the body's lipid and sphingolipid homeostasis.

Ceramides

Ceramides are sphingolipid molecules composed of an N-acylated sphingosine and a fatty acid chain that provide the backbone of all sphingolipids. These N-acylated sphingolipids do not consist of any head groups and its only R group is a hydrogen atom. The acyl chain can vary in length, with long-chain (C16) and very long-chain (C24) being the most predominant in mammalian tissue. Due to the differing lengths of acyl-CoAs that are used in production, ceramides are considered a class of molecules rather than a single molecule itself of varying forms (Gault et al., 2011), giving rise to the concept of differing biological functions which are dependent upon the different chain lengths.

Ceramide accumulation at the mitochondria can inhibit telomerase, leading to irreversible cell cycle arrest and potentially apoptosis (Hannun and Luberto, 2000; Pettus et al., 2002). Hannun and Luberto also noted that simply increasing the concentration of intracellular ceramides can induce those same stress responses in the cell. Zheng et al., in 2006, had also cited studies that had shown the induction of autophagy via addition of exogenous ceramides and sphingolipids. Generally, long-chain ceramides (especially C_{16}-ceramide) are considered to be pro-apoptotic while very long-chain are anti-apoptotic (Mesicek et al., 2010). That balance is important in order to maintain homeostasis and a shift from C_{24}- to C_{16}-ceramides has caused an increase in apoptotic activity in HeLa cells (Sassa et al., 2012). *De novo*-generated C_{18}- and C_{16}-ceramides have been observed to play significant roles regarding apoptosis regulation (Senkal et al., 2010). Mesciek et al. have shown that $C_{16:0}$-ceramide is involved in regulating apoptosis with homeostasis maintained by balancing C_{16}- and $C_{24:1}$-, $C_{24:0}$-ceramides. In that same 2010 study, ionizing radiation-

induced $C_{16:0}$-ceramide generation via ceramide synthase 5 was pro-apoptotic whereas IR-induced $C_{24:1}$- and $C_{24:0}$-ceramides via ceramide synthase 2 were pro-survival.

Ceramide synthases

Ceramide synthesis comes about in two ways (Figure 1): by hydrolysis of sphingolipids via sphingomyelinase (SM) into their constituent parts or *de novo* synthesis with ceramide synthases (CerS) in the ER via the formation of an amide bond between a sphingoid base and a fatty acyl-CoA chain (Sassa et al., 2012). Ceramide synthases were initially called Lass proteins ("Longevity assurance") due to their similarity in structure to LAG1p (Longevity assurance gene-1) in yeast. CerS are membrane-spanning proteins of a proposed odd number of transmembrane domains that utilize acyl-CoA's of differing lengths for one of six possible isoforms and are found throughout the body, though there has been little proven correlation between mRNA levels and enzymatic activity (and therefore corresponding sphingolipid distribution). Regarding the differing acyl-CoA chain lengths, long-chain (C_{16} to C_{18}) and very long-chain (C_{20} to C_{24}) are predominant in most mammalian tissues (Sassa et al., 2012) and it has been postulated that these enzymes may exhibit stereospecificity toward their sphingoid base of choice (Mullen et al., 2012).

Figure 1: Ceramide synthesis comes about in two ways. Ceramide synthesis occurs at the cytoplasmic leaflet of the ER through the *de novo* pathway or the sphingosine recycling pathway. The *de novo* pathway begins with the condensation of a serine and a fatty acyl-CoA via serine-palmitoyl transferase (SPT) to 3-ketosphingosine (3KSa). 3KSa is then reduced to sphinganine via 3-ketosphingosine reductase (3-KSR) and then N-acylated to dihydroceramide before being desaturated to ceramide. The recycling pathway occurs when sphingomyelin undergoes hydrolysis via sphingomyelinase (SM) into ceramide. Ceramide degradation via ceramidases (not pictured) is the major source of intracellular sphingosine.

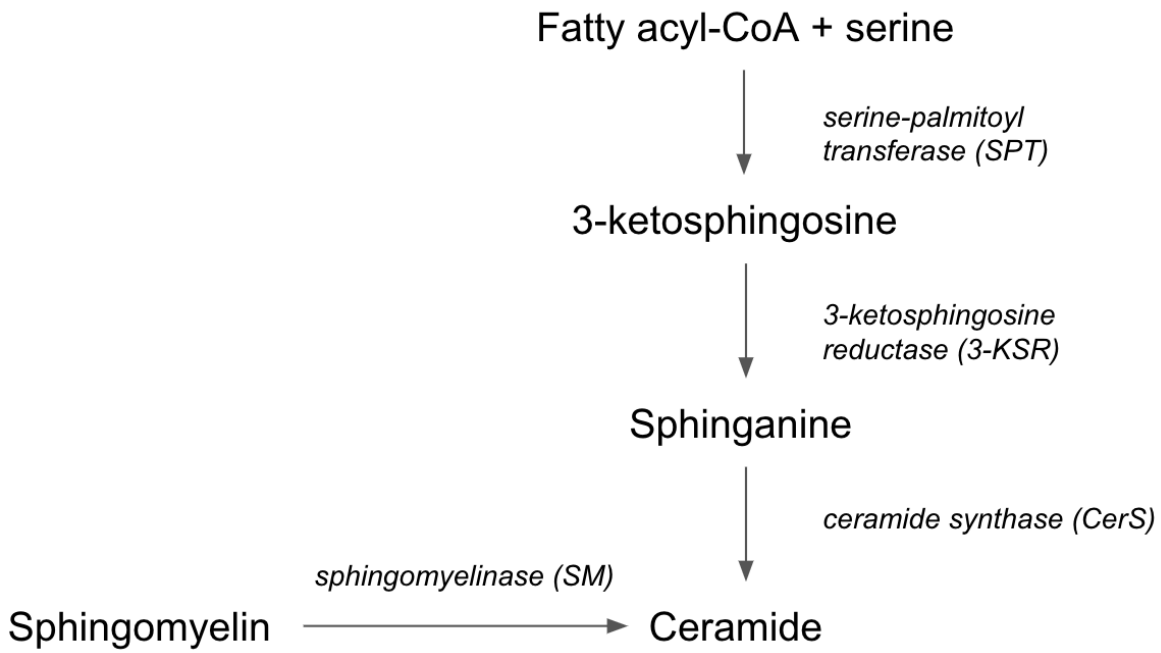

Regarding enzyme localization, *de novo* ceramide synthesis will begin in the ER and continue in the Golgi apparatus, which Pettus et al. noted in 2002 via fluorescence and time-lapse confocal microscopy. They found that ceramides form within the perinuclear region, ER, and mitochondria before accumulating in the Golgi to be metabolized further into glucosylceramide and sphingomyelin. CerS activity has been characterized within the ER (finding that enzymatic activity is available from the cytosolic leaflet of the ER) and mitochondria, but not the Golgi apparatus unless placed under stressors to force translocation of certain isoforms (Mullen et al., 2012). Those same researchers saw that CerS2 will translocate but neither CerS4 nor CerS5 behaved in that way under those same conditions.

As mentioned previously, CerS can be classified as one of six isoforms, appropriately designated CerS1 through 6. Of these six, CerS2, CerS5, and CerS6 were of interest to this project.

Ceramide synthases 2, 5, and 6

Not much is currently known about the regulation of CerS, though previous research has shown that they rapidly form homo- and heterodimers, showing a significant increase in activity level upon formation. CerS2 has been shown to be able to immunoprecipitate with CerS5 and CerS6 (Laviad et al., 2012; Mesciek et al., 2010) and has shown the highest relative increase in enzymatic activity upon dimerization. CerS5 expression has been found to be influenced by the availability of other CerS, in that depletion of CerS2 or CerS6 has increased CerS5 expression (Wegner et al., 2016). The

exact mechanisms for formation of dimers is still unknown, though a model has been developed in which the isoforms may bind to one another in order to form heterodimers that can then interact allosterically with fellow dimers or with other monomers (Laviad et al., 2012; Mesciek et al., 2010). Of the six isoforms, the regulatory mechanisms of CerS2 and CerS5 are the best understood whereas little is known about CerS6.

Wegner et al. showed that a knockdown of CerS2 was accompanied by an increase in CerS6 expression, fueling the theory that homeostasis depends upon a balance between LC and VLC ceramides. Senkal et al. in 2010 found that downregulation of CerS6 caused a decrease in C_{16}-ceramide generation with a compensatory increase in C_{22}- and C_{24}-ceramide levels.

CerS5 and 6 share approximately 61.7% identity and 68.2% similarity (Mizutani et al., 2005), catalyze the same length acyl-CoA's (C_{14} to C_{16}), and prefer palmitoyl-CoA as their main substrate, but are concentrated within different tissues and therefore found at different distributions throughout the body. CerS5 mRNA is strongly expressed in muscle and brain, with highest detection being in gray and white matter cells, as well as being majorly present in lung epithelia. In the heart, CerS5 has been shown to be required for cardiomyocyte hypertrophy and autophagy (Russo et al., 2012). The ceramides generated by CerS6, on the other hand, have been shown to play a role in ER stress-induced apoptosis as well as mitochondrial fragmentation via binding to MFF. CerS6 has been shown to be highly expressed in kidney and brain, though there has been little to no detection within muscle, spleen, or stomach (Mizutani et al., 2005).

Hypothesis

The formation of protein dimers has been well observed in nature, with many enzymes forming homo- or heterodimers in order to upregulate their activity or improve their efficacy. Ceramide synthases are no different, though a lot of their regulation and mechanisms still remain unknown. In this project, we wanted to focus on how CerS2 heterodimerizes with CerS5 or CerS6 and how that drove expression of the constituent parts. We believed that the heterodimers would indeed give way for optimal CerS2 enzymatic activity and expression, based upon proposed regulatory mechanisms and previous research conducted on the proteins. We believed that CerS2 forming a heterodimer with either CerS5 or CerS6 would drive CerS2 expression above its baseline at both the mRNA and protein levels. With the Duolink Proximity Ligation Assay, we believed that we would see puncta with both co-transfection conditions, which would indicate an interaction between the two proteins of interest, CerS2 and either CerS5 or CerS6. We also believed that CerS2 heterodimers with either CerS5 or CerS6 would alter its localization to the cell via immunofluorescence.

Materials and Methods

Cell culture and reagents:

Human and rat ventricular cardiomyocytes (AC16 and H9c2) were obtained from the Jackson Laboratory, thawed, and grown out to be utilized for this experiment. AC16 cells were grown in DMEM/F12 (Sigma Cat. No. D6434) containing 2 mM L-Glutamine (EMD Millipore Cat. No. TMS-002-C), 12.5% Fetal Bovine Serum (EMD Millipore Cat. No. ES-009-B), and 1% 1X Penicillin-Streptomycin Solution (EMD Millipore Cat. No. TMS-AB2-C) at 37°C in a 5% CO_2 atmosphere. AC16 cells were to be split at 70-90% confluence in a 150 cm^2 flask with 5.0 mL 0.05% Trypsin-EDTA with phenol red (Gibco). After splitting, the cells were transfected for 24 hours at 70% confluence using the Lipofectamine 3000 Kit obtained from Thermo Scientific.

H9c2 cells were grown up in DMEM/F10 (Sigma Cat. No. 30-2002) containing 12.5% FBS (EMD Millipore Cat. No. ES-009-B) and 1% 1X Penicillin-Streptomycin Solution (EMD Millipore Cat. No. TMS-AB2-C) at 37°C in a 5% CO_2 atmosphere. H9c2 cells were to be split at 50-70% confluence in a 150 cm^2 flask with 5.0 mL Trypsin-EDTA with phenol red (Gibco). H9c2 cells were transfected for 24 hours around 70% confluence utilizing the same Lipofectamine 3000 kit.

Before either of the grown cells were plated out for transfections, each well in a 6-well plate received a 22mm circular coverslip if the cells were intended to be used for either microscopy or Duolink Proximity Ligation Assay.

AC16 cells were utilized in more experiments than their H9c2 counterparts due to their faster rates of growth and higher level of availability for experiments.

Cells were checked daily and throughout each step of fixation and preparation in order to ensure that they were healthy and were not contaminated. Cells were reviewed under a light microscope in order to determine whether they were of appropriate confluence and form to be used for experiments. Confluence was estimated by the researcher after having been trained in cell health.

DNA

DNA constructs for CerS2, CerS5, and CerS6 were ordered from GenScript, transformed with bacteria via TOP10 Competent Cell kit, and streaked onto agar plates to be grown overnight. Colonies were chosen based upon opacity and thickness, picked onto a clean pipette tip, dropped into a 15 mL rounded bottom culture tube containing 3 mL LB Buffer and Ampicillin, and shaken over the course of a day. The next day, the cultures were examined and the cloudiest looking tubes were chosen. 100 µL were taken out from the chosen tubes and pipetted into a 150 mL flask of LB Buffer and Amp to be shaken overnight at 37°C. The following day, the 150 mL flask was split into three 50 mL tubes and spun at 3,000 x g for 20 minutes at room temperature to pellet each mixture before going into Maxi Prep per the QIAGEN HiSpeed Plasmid Maxi Kit (cat. no. 12662).

Before the Maxi Prep, RNase A solution was added to Buffer P1 and stored at 4°C, along with Buffer P3, both included in the kit. Bacterial pellets were resuspended in 10 mL

Buffer P1, with the first pellet receiving 10 mL, being pipetted up and down in order to mix them, then added to the next pellet of the same DNA in order to re-combine the three 50 mL's from the original 150 mL flask. Once the pellets are homogenized and in a single 50 mL tube, 10 mL Buffer P2 was added and the tube was inverted 4-6 times before being incubated at room temperature for 5 minutes. After incubation, 10 mL of Buffer P3 was added and mixed by inverting the tube again. The tube was then poured into the barrel of a QIAfilter Cartridge with a cap screwed onto the outer nozzle incubated at room temperature for 10 minutes without the plunger inserted.

During that time, a HiSpeed Tip was equilibrated with 10 mL Buffer QBT via gravity filtration. After the incubation, the cap was removed from the cartridge and the plunger was inserted, pushing out the cell lysate slowly into the HiSpeed Tip. Once the lysate had passed through the filter, the HiSpeed Tip was washed with 60 mL Buffer QC and then the DNA was eluted into a 50 mL tube with 15 mL Buffer QF.

10.5 mL isopropanol was added to the DNA for precipitation, mixed and incubated at room temperature for 5 minutes. During that time, a plunger was removed from a 30 mL syringe and screwed onto a QIAprecipitator Module. The QIAprecipitator and plunger was placed over a waste bin and the eluate-isopropanol mixture was added to the syringe and filtered through the precipitator. The QIAprecipitator was removed from the syringe in order to pull out the plunger and then reattached before adding 2 mL 70% ethanol to the syringe to wash the DNA. The precipitator was removed to pull out the plunger and then reattached before inserting the plunger and pressing air through the precipitator to dry the membrane. The QIAprecipitator was then moved onto a 5 mL syringe and held over a 1.5

mL collection tube. 1 mL Buffer TE was added to the syringe and pushed through to elute the DNA into the 1.5 mL collection tube. That last step was repeated in order to maximize DNA concentration. That DNA was then used for transfections.

Transfections

Each transfection condition's mastermix was initially mixed in two different tubes before they were combined. The first set of mastermixes was composed of, per well, 125 µL Opti-MEM Reduced Serum Media (Thermo Fisher) and either 3.75 or 7.5 µL of Lipofectamine 3000. Transfections of CerS2 and CerS6 as well as co-transfections of CerS2 with CerS5 and CerS2 with CerS6 were accomplished with 7.5 µL of lipofectamine whereas pcDNA and CerS5 both utilized 3.75 µL of lipofectamine. The second set of mastermixes was 125 µL of Opti-MEM, 5 µL of p3000, and 5 µg of DNA for each transfection condition. After allowing the DNA mixture to sit for approximately 10 minutes, the two tubes were mixed and an equal amount was pipetted into each appropriate well. Each well also received a media change prior to transfection. The transfection media sat for 24 hours and then was removed prior to fixation or cell processing.

Co-localization microscopy experiments

After the 24 hour transfection, the media was removed from each well before 2 mL of -20°C methanol was added and the plate was put into a -20°C freezer for 15-30 minutes. Then, at room temperature, the methanol was removed and each coverslip was blocked in 5% BSA Fraction V-1X PBS with 10 mM glycine and 0.1% Triton-X for 30 minutes.

Antibodies (Lass2 C-11 from Santa Cruz, sc-390745, raised in mouse; Lass5 PA5-20569 from Thermo Scientific, raised in rabbit; Lass6 PA5-20648 from Thermo Scientific, raised in rabbit) were diluted to 1:100 in 1% BSA Fraction V-PBS-gly. Lass2 had to be raised in a different animal to Lass5 and Lass6 in order to best utilize immunofluorescence to determine co-localization. The blocking solution was removed and 50 µL of the antibody solution was placed on a clean sheet of parafilm onto which each corresponding coverslip was flipped. The coverslips were incubated for 30 minutes at room temperature. The coverslips were incubated for 30 minutes at room temperature, flipped back into a clean 6-well plate with the cell side up, and then washed three times with 1X PBS for five minutes each. Secondaries (goat anti-mouse fluor 488 and chicken anti-mouse fluor 594, both obtained from Thermo Scientific) were diluted to 1:400 in the same 1% BSA Fraction V-PBS-glycine. 50 µL of the secondaries were pipetted onto a new sheet of clean parafilm onto which the now washed slides were flipped. The coverslips were incubated in the dark for 30 minutes then washed again with 1X PBS for five minutes each. The coverslips were then mounted with a drop of 10 mM n-Propyl gallate in glycerol, the excess was lightly dabbed off with a Kimwipe, and sealed with clear nail polish. The slides dried for approximately 30 minutes in the dark before they were stored at 4°C to the imaged the next day.

Duolink Proximity Ligation Assay

After 24 hour transfections, the media was removed from each well and each coverslip received approximately 2 mL of 4% paraformaldehyde and sat at room

temperature for 15 minutes for cell fixation. The PFA was removed then the coverslips were quenched with three 1X PBS-glycine washes for five minutes each. A clean piece of parafilm was cut to size and a droplet of the blocking solution included in the Duolink PLA kit was added for each coverslip. Coverslips were inverted over the droplet so the cell side faced the droplet and each slip was incubated for 30 minutes in a 37°C chamber. During this time, primary antibodies (the same Lass2, Lass5, and Lass6 used in co-localization immunofluorescence experiments as well as COX4 for a mitochondrial marker) were diluted in combinations of Lass2 and Lass5 or Lass6 (all being combined with COX4) at 1:50 in the antibody diluent included in the Duolink PLA kit. After the 30 minute incubation, 50 µL of the antibody solution was pipetted onto another clean sheet of parafilm and coverslips were placed onto each drop to sit at room temperature for two and a half hours.

After primary antibody incubation, coverslips were washed twice for five minutes each with room temperature Buffer A (0.88% NaCl, 0.12% Trizma Base, 0.005% Tween, all from Sigma Aldrich, water to 1 L, pH 7.4, filtered through 0.22 µm filter paper via gravity filtration). PLA secondary anti-rabbit plus and anti-rabbit mouse minus probes, included in the Duolink secondary kits, were diluted at 1:5 with the same antibody diluent for primary antibodies. Chicken anti-goat fluor 488 secondary antibody was diluted at 1:400 and mixed with the PLA probe solutions Approximately 40 µL were pipetted onto a clean sheet of parafilm for each coverslip, onto which each slip was flipped over and then incubated in a 37°C chamber for one hour.

Toward the end of the hour for the PLA probe incubation, ligation stock from the Duolink *in situ* Detection Reagents kit from Sigma Aldrich was diluted 1:5 with nuclease-free water. Ligase from the same kit was diluted 1:40 in that ligation-water solution. The coverslips were taken off the parafilm and placed into a clean 6-well plate cell side up for two Buffer A washes for five minutes each. 30 µL of the ligation-ligase was pipetted onto clean parafilm onto which each coverslip was flipped and then incubated for 30 minutes at 37°C.

As the ligation reaction incubation period ended, AMP stock from the Duolink *in situ* Detection Reagents kit was diluted 1:5 with nuclease-free water. Polymerase from that same kit was added at 1:80 to the AMP solution. The coverslips were removed from the parafilm and put into a clean 6-well plate for two Buffer A washes at two minutes each. 40 µL of the AMP-polymerase solution were pipetted onto clean parafilm and slips were incubated at 37°C in the dark for 100 minutes. After the incubation, slips were flipped back into the 6-well plate for two room temperature Buffer B (0.584% NaCl, 0.424% Trizma Base, 2.6% Tris-HCl, all from Sigma Aldrich, water to 1L, pH 7.5, filtered through 0.22 µm filter paper via gravity filtration) for ten minutes each. The slips were then washed once in 0.01X Buffer B diluted with nuclease-free water, for one minute each. Coverslips were mounted with 1 µL of Duolink Mounting Medium with DAPI and sealed with clear nail polish. Slides were left to dry in the dark for approximately 30 minutes before being stored at 4°C to be imaged the next day.

Confocal microscopy

All microscopy images were taken on a Zeiss LSM 700 microscope. All microscope operators were trained on the microscope prior to first usage and had a practice run in which they would take slide images with a microscopy faculty member. Both co-localization immunofluorescence and Duolink experiments were evaluated using confocal microscopy. Laser intensities and gain were set with a positive set at the beginning of the microscopy session, checked against the negative controls, and then were not adjusted throughout an imaging set. All images were taken on 63x oil objective. Microscopy was performed at the VCU Microscopy Facility, support part, by funding from NIH-NCI Cancer Center Support Grant P30 CA016059.

Protein processing and western blots

AC16 cells were split into 6-well plates without coverslips and were transfected as described previously once the cells reached appropriate confluence. After the 24 hour transfection, the media was removed and 100 µL of RIPA+PPI were added to each well in order to solubilize the cell layer for scraping to remove the protein. Each tube received a hard spin at 10,000 x g for 15 minutes at room temperature. Protein concentration was determined via BCA assay (kit from Thermo Scientific) with the samples diluted at 1:10 in RIPA+PPI and read at 460 nm. Readings were normalized to four standard: 0 µg/µL, 500 µg/µL, 1000 µg/µL, and 2000 µg/µL. Protein was then diluted with RIPA in order to reach 1 µg/µL and 4x Laemmeli diluted 3:4 with betamercaptoethanol to reach 200 µL total volume. The samples were boiled for five minutes before being loaded into a 10%

Criterion Stain-Free precast electrophoresis gel from Bio-Rad and run at 225V for 30 minutes immersed in 1X Running Buffer. Gels were then removed from the plastic casing, activated via Bio-Rad imager, and transferred onto a PVDF membrane for ten minutes. Blots were blocked in 5% FAF BSA in TBST for 30 minutes on a rocker at room temperature and the same Lass antibodies as previously mentioned for microscopy experiments were diluted 1:1000 in the same 5% BSA-TBST as the blocking solution. The antibody dilutions were applied to each appropriate blot after blocking and blots were incubated at 4°C overnight on a rocker.

The next day, blots were brought to room temperature for an hour before being washed thrice with 1X TBST for ten minutes at a time. The same fluorescent secondary antibodies as the microscopy experiments were diluted 1:2000 in 5% BSA-TBST and applied to each blot, which sat at room temperature in the dark on a rocker for an hour. The blots were then washed thrice once more before image capture on the Bio-Rad imager.

RNA, cDNA, and qPCR

AC16 cells were grown up in 6-well plates without coverslips and transfected when they reached appropriate confluence. After the 24 hour transfection period, the media was removed and each well received 1 mL Trizol to be pipetted into appropriately labeled tubes. RNA isolation began with a room temperature incubation of the homogenized samples for five minutes to allow for complete dissociation of nucleoprotein complexes. 0.2 mL of chloroform per 1 mL of Trizol was added to each tube, which were then shaken vigorously by hand for 15 seconds before another room temperature incubation for two to

three minutes. The tubes were then centrifuged at 12,000 x g for 15 minutes at 4°C for the mixture to separate into a lower red phenol-chloroform phase, an interphase, and a colorless upper aqueous phase that contained the RNA.

That aqueous phase was transferred to a fresh tube and the remaining organic phase and interphase were discarded. The RNA was precipitated from the aqueous solution via the addition of 0.5 mL isopropyl alcohol per 1 mL of Trizol used for initial homogenization. Up to 700 µL of the sample was transferred to an RNeasy Mini spin column placed into a collection tube at a time, before being centrifuged for 15 seconds at 10,000 x g. The flow-through was discarded and that step was repeated for any remaining sample. 700 µL of Buffer RW1, included in the RNeasy kit, was added to the spin column and the tubes were centrifuged for 15 seconds at 10,000 x g, again discarding flow-through. 500 µL of Buffer RPE was added, the tubes were centrifuged for 15 seconds at 10,000 x g, and flow-through was discarded. The step was repeated with the amount of RPE, though the tubes were then centrifuged for two minutes at that same speed. The RNeasy spin column was then placed into a new 2 mL collection tube and centrifuged at 10,000 x g for one minute to dry the membrane. The RNeasy column was then placed into a new 1.5 mL collection tube and 35 µL of RNase-free water was added directly to the membrane without contacting it. The tubes sat at room temperature for ten minutes before being centrifuged for a minute at 10,000 x g to elute the RNA.

RNA concentration was measured via Nanodrop in order to determine the amount of RNA, nuclease-free water, and iScript solution to reach 250 ng/µL at a final volume of20 µL in 0.5 mL tubes. The new tubes were placed in the thermal cycler and processed

per the iScript program for cDNA creation. cDNA is a term that describes an mRNA transcript's sequence that is expressed as DNA bases, rather than RNA bases. cDNA probes only contain exons and does not include the introns that were spliced out during translation from DNA to mRNA. Once the program finished, the samples were diluted with 180 µL of nuclease-free water and kept at -80°C for long-term storage.

qPCR mastermixes were comprised of, in µL/tube, 10 µL SYBR Green from Bio-Rad, 7 µL nuclease-free water, 2 µL of 10 mM forward and reverse primer solution, and 1 µL of 2.5 ng cDNA. Primers for qPCR were hGAPDH, hCerS2, hCerS5, and hCerS6 from Thermo Scientific. Each plate was a different primer in order to minimize confusion and samples were done in triplicate. Samples were laid out in the following order: Untransfected, pcDNA, hCerS2, hCerS5, hCerS6, hCerS2 and hCerS5 co-transfection, hCerS2 and hCerS6 co-transfection. After normalization with the four standard amounts, qPCR results were analyzed and graphed per an Excel ddC_t algorithm, which is utilized in order to measure relative changes in gene expression compared to that of the reference gene. The y-axis of each qPCR graph represented fold change of the level of cDNA in each sample when run with a specific primer and acts as a method to analyze the relative changes in each gene's expression.

Results

CerS co-overexpression drives expression of the CerS species at the mRNA level

qRT-PCR, or simply qPCR, is an experimental tool used in order to measure the level of gene expression in a cDNA sample. The AC16 samples run were untransfected (abbreviated to UT) and pcDNA as the two negative controls versus the experimental transfection conditions: CerS2, CerS5, CerS6, CerS2 co-expressed with CerS5 (abbreviated to CerS2+5), and CerS2 co-expressed with CerS6 (abbreviated to CerS2+6). The primers run were each 10 mM mixtures of forward and reverse hGAPDH, hCerS2, hCerS5, and hCerS6. Figure 2A shows that hGAPDH was an appropriate housekeeping gene in that each sample's cDNA level is equal and their expressions do not exhibit any fold change.

qPCR, in this project, not only confirmed the respective identities of the DNA constructs that were utilized for transfection but also showed that co-transfection of CerS2 with either CerS5 or CerS6 drove gene expression more compared to that of its individual transfection. The hCerS2 primer showed that CerS2 and the two co-transfections had the highest levels of cDNA gene expression with CerS2 around 2000, CerS2+5 around 3000, and CerS2+6 around 11000 fold change compared to those levels in hGAPDH (Figure 2B). The qPCR showed that CerS2+6 does drive CerS2 expression to a much higher extent than that of CerS2+5. The hCerS5 and hCerS6 primers (Figure 2C and 2D, respectively) showed a similar result, though hCerS5 had significantly lower fold changes, as represented by the smaller range of its y-axis in Figure 2C, which may be due to the

differing binding affinities of these qPCR primers. CerS2+6 had approximately a 200-fold change over CerS6 alone, which does still show an increase in gene expression though maybe not a significant one, given that the CerS6 sample alone already showed a 1300 fold change compared to that of hGAPDH.

Figure 2: Co-transfections of two CerS isoforms will drive gene expression levels. (A) hGAPDH acted as an appropriate reference gene for this set of qPCR's, as shown by the consistent and low expression levels throughout all samples, including the two negative controls. They were all even and equal. Results for the three experimental primers were normalized to these values. (B) With hCerS2, it was very clear that the co-transfection of CerS2 and CerS6 (CerS2+6) drove CerS2 expression almost 8000-fold over the expression of CerS2 alone. The co-transfection of CerS2 and CerS5 (CerS2+5) also increased CerS2 levels by about 1000-fold, showing that co-transfections with both CerS5 and CerS6 can allow CerS2 to dimerize and upregulate its level of cDNA. (C) The level of fold change of hCerS5 expression compared to that of hGAPDH is lower than that of the other primers, but CerS5 still has at least a 10-fold change above the two negative controls. As was seen with the hCerS2 primer, CerS2+5 increased the level of gene expression by 70-fold. (D) The CerS6 solo transfection had a very strong level of expression, with the CerS2 and CerS6 co-transfection being about 100-fold higher.

A.

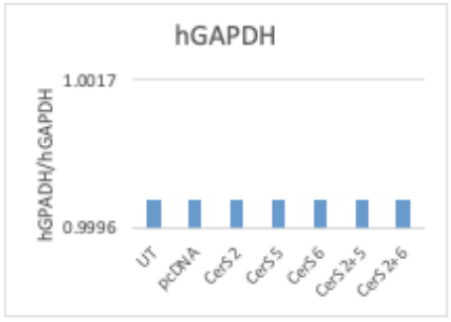
hGAPDH
1.0017
0.9996
hGPADH/hGAPDH
UT
pcDNA
CerS 2
CerS 5
CerS 6
CerS 2+5
CerS 2+6

B.

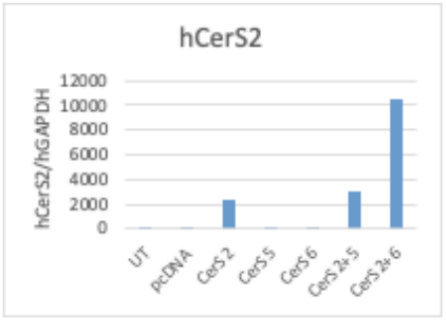
hCerS2
12000
10000
8000
6000
4000
2000
0
hCerS2/hGAPDH
UT
pcDNA
CerS 2
CerS 5
CerS 6
CerS 2+5
CerS 2+6

C.

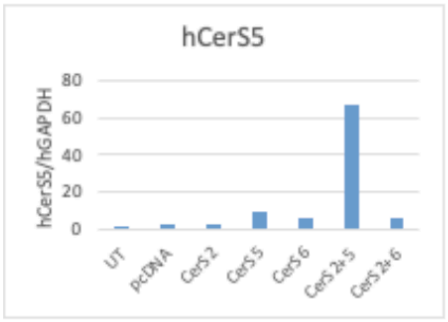
hCerS5
80
60
40
20
0
hCerS5/hGAPDH
UT
pcDNA
CerS 2
CerS 5
CerS 6
CerS 2+5
CerS 2+6

D.

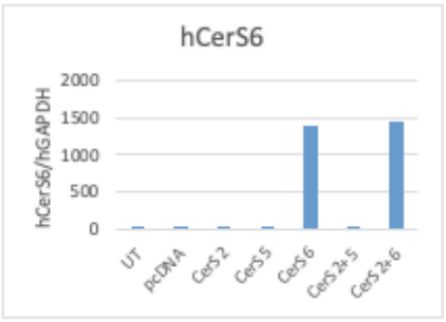
hCerS6
2000
1500
1000
500
0
hCerS6/hGAPDH
UT
pcDNA
CerS 2
CerS 5
CerS 6
CerS 2+5
CerS 2+6

CerS2 localizes differently compared to CerS5 and CerS6

AC16 coverslips were transfected and prepared for immunofluorescence experiments with images taken on a confocal microscope. AC16 cells were primarily used for these localization experiments due to their higher rate of growth and therefore their larger availability. Laser strengths were set via individual transfection conditions (Figure 4) and then checked against negative controls (Figure 3) in order to confirm that the last intensities were appropriate. Images were taken on a confocal LSM 700 microscope at 63x oil objective. Exposure to all confocal microscope images was increased by approximately 30% after image capture to improve clarity.

Figure 3: Negative controls for localization immunofluorescence. This set of images and experiments served as the negative controls for the localization and co-localization immunofluorescence experiments. (A) Both untransfected and pcDNA slides underwent the same immunofluorescence protocol as the experimental conditions but did not receive any primary antibody. This is to test for secondary antibody specificity and to see if there was any background noise that needed to be corrected. (B), (C) Five untransfected and pcDNA slides, respectively, underwent that same immunofluorescence protocol in order to mimic what was being performed on the experimental condition slides. Confocal laser settings were not changed between slides.

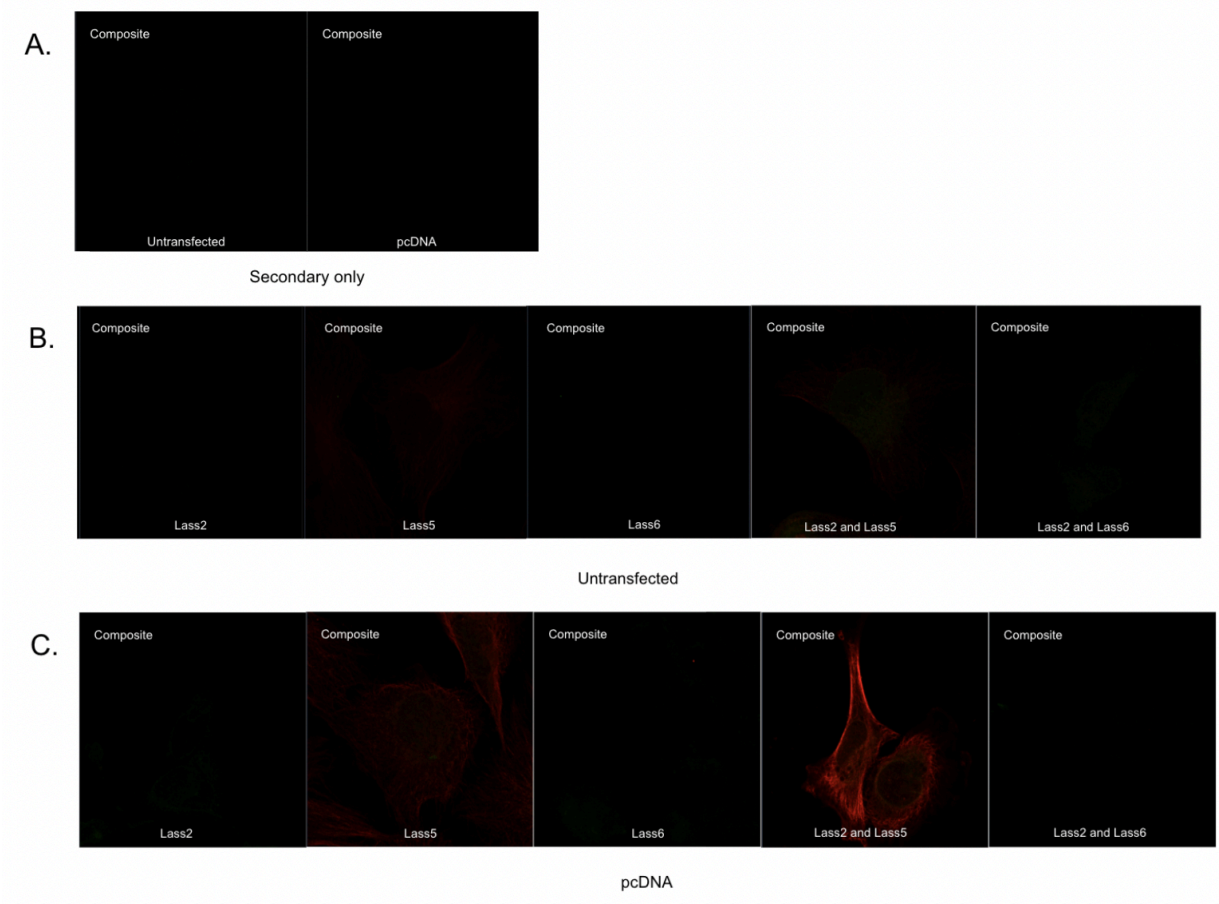

The experimental condition slides ultimately showed that CerS2 does localize to the cell differently when compared to CerS5 or CerS6 (Figure 4A). When transfected individually, the CerS isoforms also seem to have different degrees of fluorescence intensity. All CerS isoforms have been previously shown to localize to the ER and the CerS2 slide does show exactly that, along with an area of brighter immunofluorescence that looks to be localized to the Golgi apparatus. Even when co-transfected with CerS5 or CerS6, that Golgi bright spot remains, potentially being a result of CerS2 possibly being glycosylated in the Golgi. Neither CerS5 nor CerS6 had that same area. Past AC16 slide preparations and imaging have shown a similar bright area in the same region. H9c2 cells were not utilized for this experiment due to low availability and time constraints.

CerS5 and CerS6 both showed a strong juxtanuclear staining pattern when transfected individually. CerS5 seemed to localize to both the ER as well as the mitochondria, given the prominent web-like pattern extending outwards from the nucleus. CerS6 had the same fluorescence intensity as that of CerS5. The differences in the CerS5 and CerS6 localizations when compared to that of CerS2 and each other may be a result of undergoing different post-translational modifications at the time of cell fixation. MitoTracker would have been a helpful tool in order to truly determine localization to the mitochondria though it was not included in this experiment due to time constraints and should absolutely be a consideration for any future iterations of this project.

Co-transfected AC16 cells are shown in B and C of Figure 4. The constructs and antibodies utilized remained the same throughout all the localization experiments. In both co-transfections, CerS2 still has a bright area in the region of the Golgi that is not present

in either CerS5 or CerS6. In 4B, the CerS2 displays a much bright immunofluorescence compared to that of CerS5 as well as to the individual CerS2 transfection. Regarding any true co-localization, there does seem to be one spot in CerS2+6, indicated by an arrow.

Figure 4: CerS2 localizes differently to the cell compared to CerS5 and CerS6. Confocal microscopy images were altered to an increased exposure of approximately 30%. Green represents the anti-mouse secondary for the Lass2 antibody (488 fluor) while red represents the anti-rabbit secondary used for Lass5 and Lass6 (fluor 555). (A) Each of the individual transfections were treated with their respective antibody and imaged. CerS2/Lass2 does shown a different pattern and level of intensity of fluorescence compared to that of CerS5/Lass5 and CerS6/Lass6, which share similar staining patterns. (B) and (C) The co-transfections confirmed that CerS2 did localize differently when compared to its sister isoforms. The purple arrow in (C) indicates an area of co-localization, as shown by the yellow coloring of the area of overlap.

A.

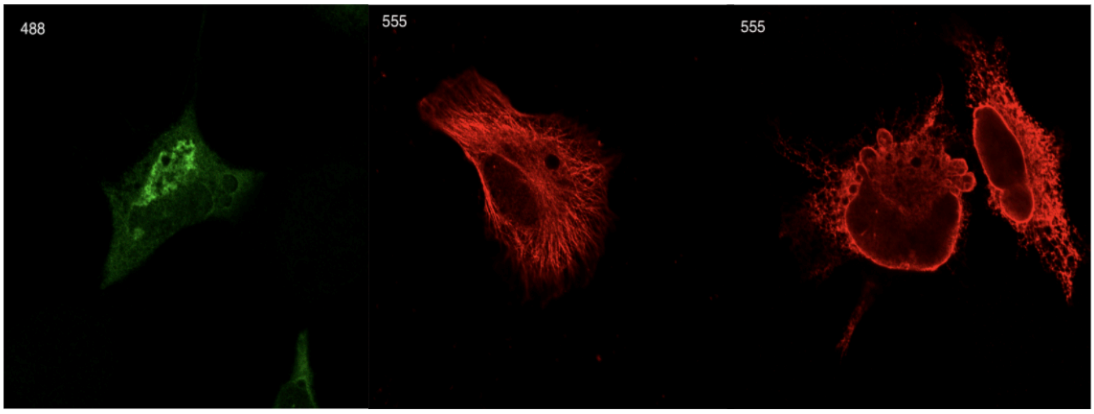

hCerS2 transfection, Lass2 ab | hCerS5 transfection, Lass5 ab | hCerS6 transfection, Lass6 ab

B.

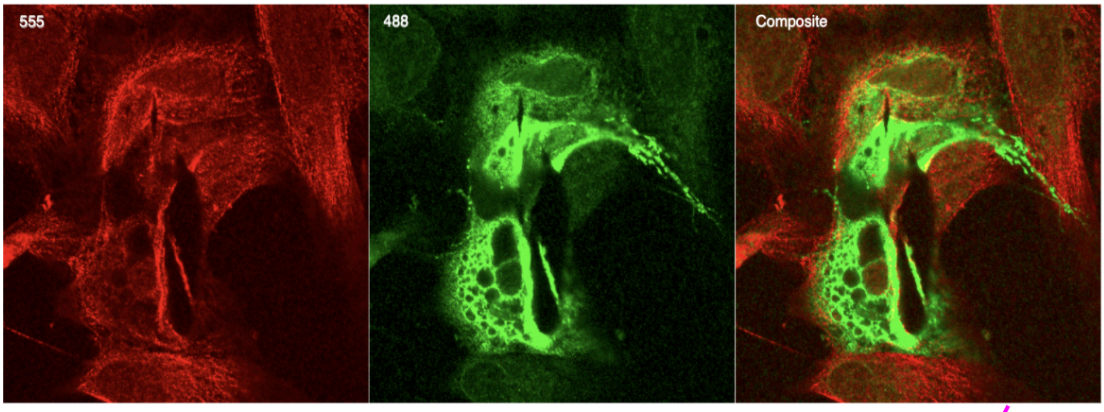

hCerS2+5 transfection, Lass2 and Lass5 ab

C.

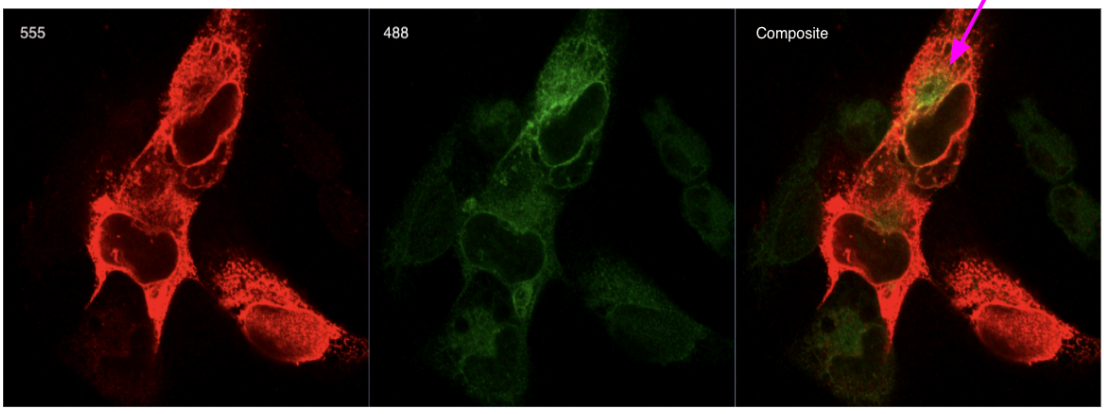

hCerS2+6 transfection, Lass2 and Lass6 ab

Endogenous CerS do not interact in H9c2 cells but do in AC16

Duolink *in situ* fluorescence Proximity Ligsation Assay was utilized in this experiment for its high specificity and sensitivity regarding detection of endogenous protein interactions as well as protein expression levels at the molecular level. Both AC16 and H9c2 cells were treated in the same manner and underwent the same protocol simultaneously. Images were taken on a confocal microscope at 63x oil object and images have been altered for clarity by increasing exposure by approximately 30%. However, no puncta were seen in the H9c2 set of slides, as seen in Figure 5. That lack of puncta indicates that the proteins of interest were not within 40 nm of each other and therefore could not interact with the PLA probes. Even the co-transfections did not reveal any puncta in the H9c2 cells. COX4 G-20 antibody was utilized as a mitochondrial marker for the Duolink slides.

Figure 5: Puncta were not seen in Duolink with H9c2 cells. Blue represents the DAPI nuclear staining contained within the mounting medium used for these slides. Green represents the COX4 antibody used as a mitochondrial marker. The staining pattern was not represented evenly in all coverslips, possibly due to the use of PFA as the fixation reagent. (A) The negative controls, Untransfected and pcDNA, treated with both antibody combinations and having undergone the entirety of the Duolink experimental protocol. (B) No experimental conditions, not even the co-transfections, showed puncta.

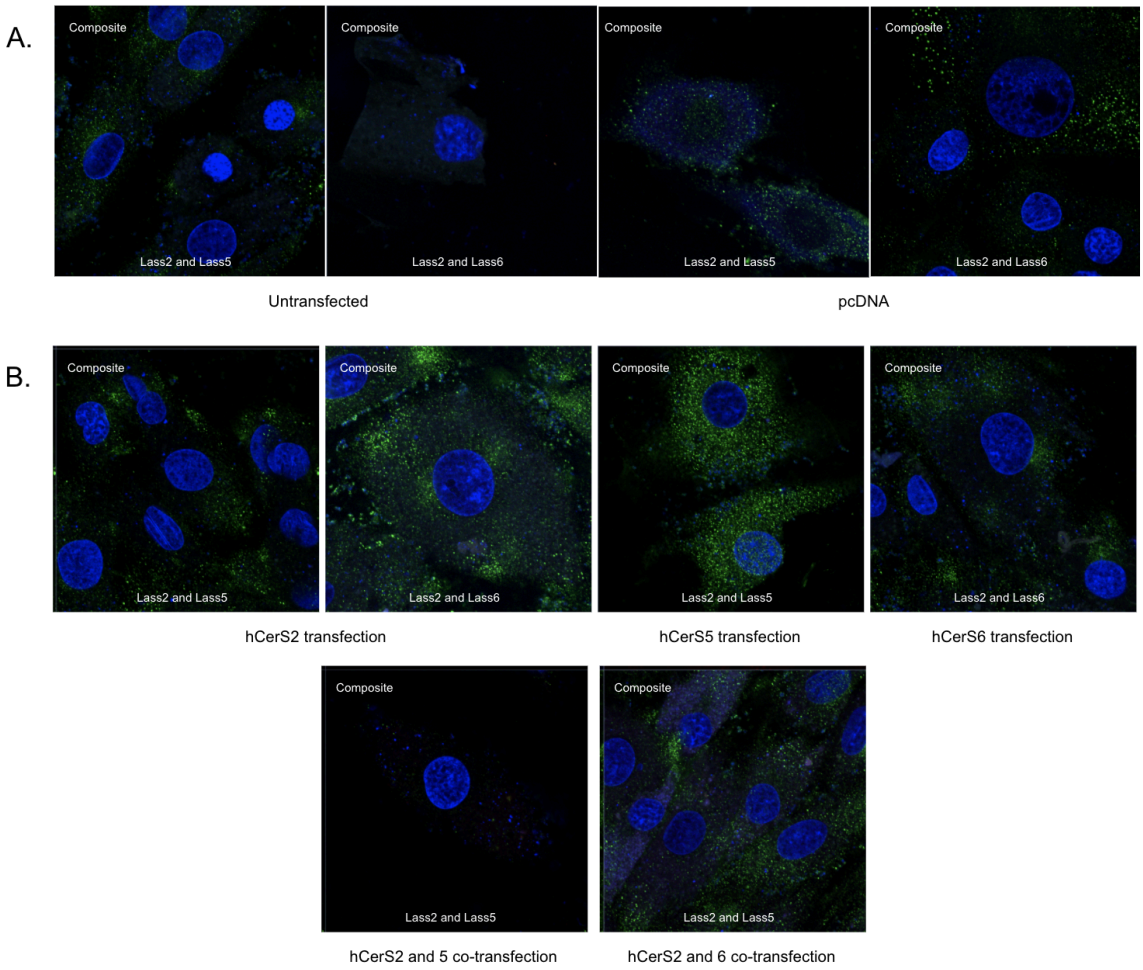

AC16 cells, however, did show puncta which would indicate that the proteins of interest (the CerS isoforms) are indeed within 40 nm of each other and would be able to interact and dimerize. As with the H9c2 cell slides, laser intensities were set using the individual transfection conditions and then checked against the negative controls to ensure that they were adequate. Figure 6 shows the negative controls for the AC16 set, this time including a slide for secondary only.

Figure 6: Negative controls for AC16 Duolink. The negative control panel utilizing Untransfected and pcDNA slides confirmed that there was no background that required correcting in the experimental sides nor were the antibodies non-specific. With the secondary only condition, it confirms that the PLA probes were specific for this experiment. Blue represents DAPI nuclear staining from the mounting media and green represents the COX4 mitochondrial staining. The pattern of the staining seems to be a result of the PFA staining, as does the unequal expression across all slides.

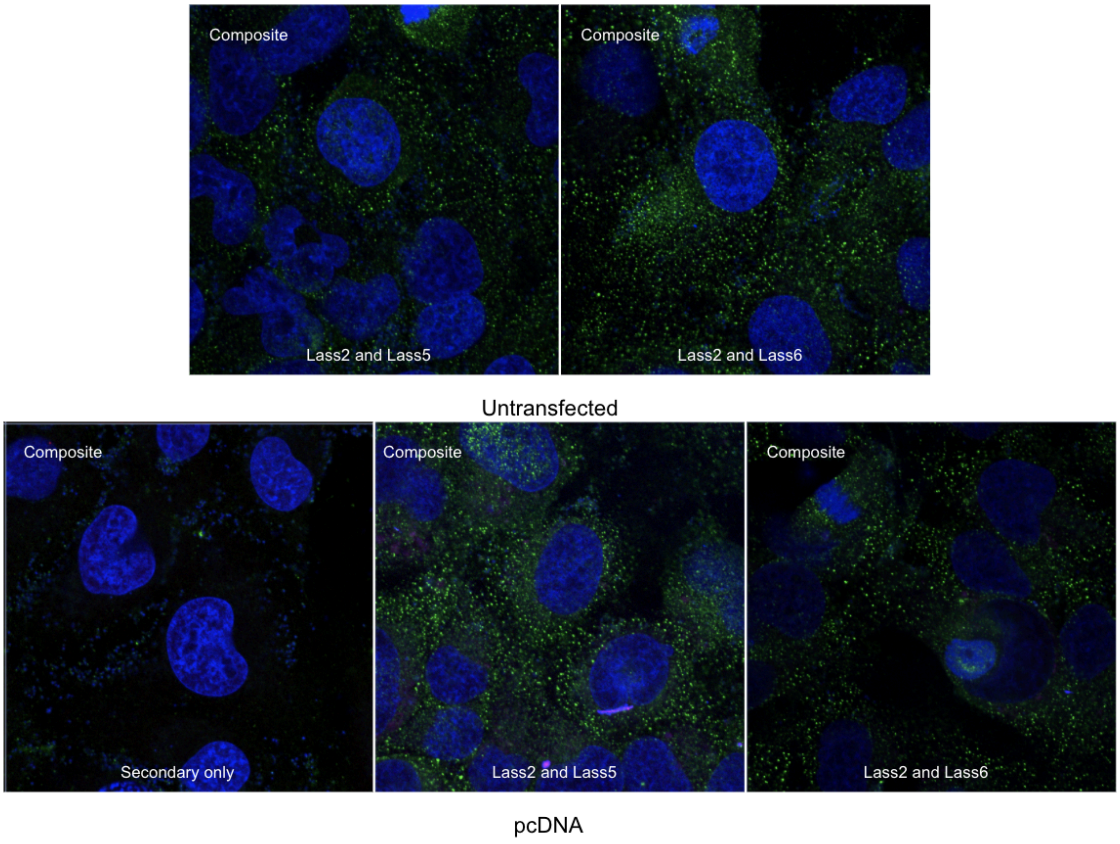

The major aspect of Duolink that differs from other forms of immunofluorescence is the usage of Proximity Ligation Assay (PLA) probes, which bind to the primary antibody and are combined with short synthetic strands of DNA. If the proteins of interest are within the 40 nm that the PLA probes allow for, these probes will then hybridize with one another to create circular DNA. The ligase will then be added to form a complete circular DNA template, which will be utilized for amplification and fluorescently-labeled visualization. The red color of the puncta come from the red dye contained within the DNA polymerase which will utilize the primer created by the PLA probes for rolling circle amplification and generate up to 1000 copies of the template. That amplification remains with the PLA probe, which allows for localization of protein-protein via puncta.

Both co-transfection conditions showed puncta (Figure 7), more so than their individual transfection cohorts, which was to be expected based upon previous research as well as what was seen during this project. The puncta seen are more strongly concentrated in CerS2+6 compared to CerS2+5, which aligns with what was seen with CerS2 mRNA in Figure 2B. Overall, the presence of puncta in both co-transfection conditions shows that these CerS isoforms not only interact at the mRNA level, but also at the protein level. Another experiment that should have been taken into consideration would have been co-immunoprecipitating CerS2 with CerS and CerS6 as Co-IP is another technique used to identify protein-protein interactions via protein-specific antibodies. Co-IP would not have been able to identify any transient protein-protein interactions in the way that Duolink can but it would have acted as a confirmation for the dimerization of CerS2 with CerS5 and CerS6 if we could have immunoprecipitated both species from the co-transfections.

Figure 7: Co-transfections of CerS2 with CerS5 or CerS6 show puncta with Duolink. Blue represents DAPI nuclear staining contained within the mounting media, green represents COX4 mitochondrial staining, and red is puncta, which indicates protein-protein interactions per the Duolink protocol. Both co-transfection conditions show puncta, which is consistent with the isoforms forming heterodimers at the cDNA levels, shown earlier by the qPCR results. The puncta is stronger in CerS2+6, another aspect that has shown to be consistent from the mRNA. The presence of puncta indicates that these CerS isoforms are interacting at the protein level in these fixed cells.

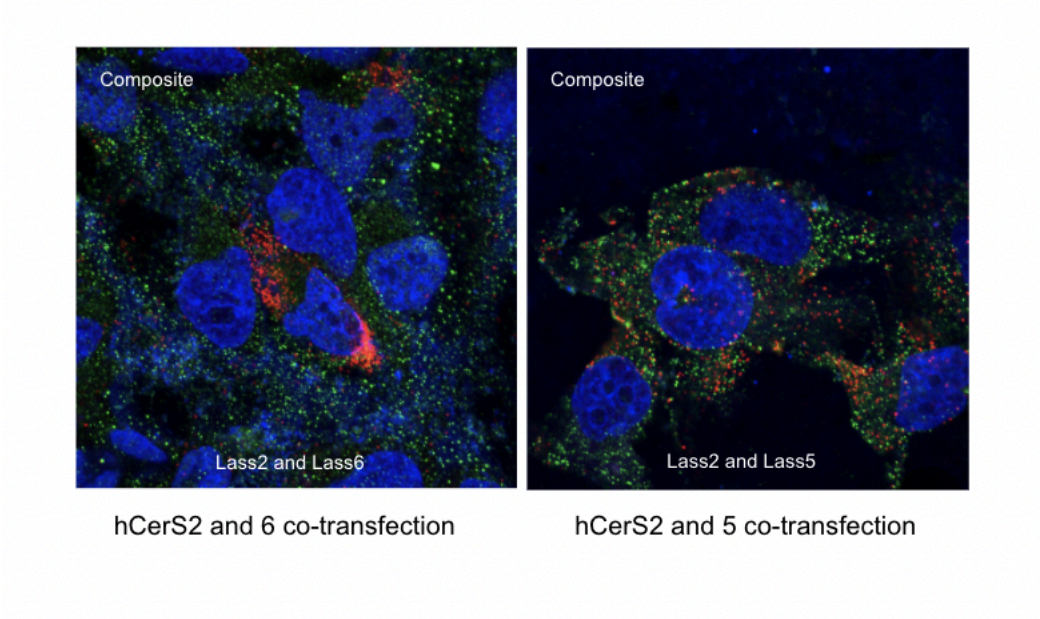

Figure 8 represents the results at the protein level of the individual CerS6 transfection. The western blot (Figure 8A) indicates that, not only was the Lass6 antibody utilized indeed specific to CerS6 and there was a bolder band in the CerS2+6 co-transfection, but also that cells overexpressing CerS2 may also be expressing endogenous CerS6 at the protein level, as indicated by a dark band in the CerS2 sample lane. As was seen in the CerS2+6 co-transfection Duolink image, CerS2+6 has the largest and darkest band in the entire blot, indicating a high level of protein present in that condition. The presence of endogenous CerS6 within cells overexpressing CerS2 could be a result of the more ubiquitous distribution of CerS2 compared to that of CerS6 and the need to be able to balance out pro- and anti-apoptotic mechanisms within each cell. As was discussed in the introduction, previous research had revealed a general rule about ceramide length and apoptosis: LC ceramides, especially C_{16}-ceramide, are typically pro-apoptotic whereas VLC ceramides are generally anti-apoptotic. CerS6 and CerS5 are the isoforms responsible for producing C_{16}-ceramides and their combined distribution still does not equate that of CerS2, so this may be a compensatory failsafe in the event that apoptosis is required in an area in which CerS5 or CerS6 is not prominent.

The expected molecular weight for these bands was around 48 kDa and the CerS2+6 band being a little higher than expected could be due to some type of post-translational modification (such as glycosylation, as was suspected with CerS2) or simply the formation of a multimer. The western blot was run at 225V for 30 minutes, which may not always be an ideal voltage for a polyclonal antibody such as this Lass6. For future experiments based upon this project, I would certainly recommend running the western

closer to 100V for at least an hour, if not longer to ensure that the bands reach the bottom of the gel.

The lack of puncta in Figure 8B would indicate that there is no interaction between CerS6 and CerS2 that may be found endogenously within cells overexpressing CerS6. There was also no green COX4 staining present, which may have been due to the use of 4% paraformaldehyde as the fixative agent rather than using a dehydrating agent such as -20°C methanol.

Figure 8: Cells overexpressing CerS6 do not show any endogenous sister isoforms. (A) The western blot indicates that the Lass6 antibody was appropriate for these experiments as there are bands in both the hCerS6 and hCerS2+hCerS6 lanes. However, there was also a band present in hCerS2, which may indicate the presence of endogenous CerS6 contained within cells overexpressing CerS2. The largest band is clearly in the hCerS2+hCerS6 sample lane, which is congruent with what was seen in the mRNA. (B) Blue is DAPI nuclear staining, found in the mounting medium. This Duolink image does not show any puncta (which would have been in red) or, interestingly enough, any COX4 mitochondrial staining (which would have been in green). The lack of puncta shows that there are no detectable protein interactions when Lass2 and Lass6 are applied to the CerS6 transfection, indicating the absence of CerS2 in cells overexpressing CerS6. The lack of green COX4 staining may be due to the PFA fixative agent or even the dilution of the secondary utilized.

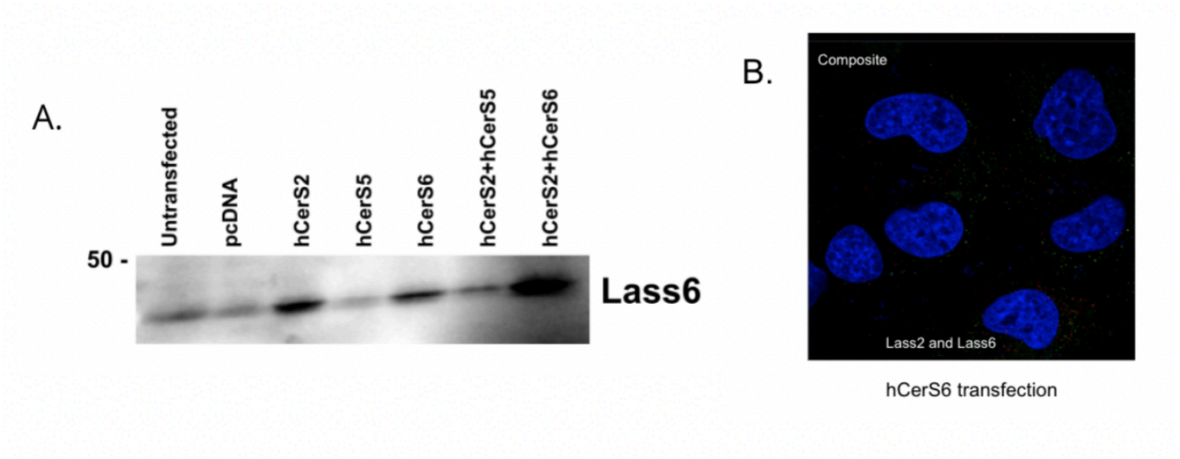

Figure 9 represents the same protein findings as Figure 8, though this time for CerS5. Similarly to CerS6, the Lass5 antibody used in Figure 9A shows an appropriate amount of specificity for CerS5 as it showed the darkest band in the hCerS5 lane. It also showed a band in the hCerS2 lane, which indicated that cells overexpressing hCerS2 contains both endogenous CerS5 and CerS6. Interestingly, the band in the hCerS2+hCerS5 lane is darker than the ones associated with the negative controls as well as the one in hCerS6, but is not larger than the one in the hCerS5 transfection condition. That discrepancy in band size does not correlate with what was seen in the mRNA, which showed a decent increase in gene expression level in the co-transfection compared to that of the individual transfection condition. This could mean that changes at the mRNA level do not translate to the protein level or could possibly be a result of human error when performing experiments. Like the other western blot, this was run at 225V for 30 minutes and was unable to be repeated due to time constraints. It would absolutely be of worth to run this blot again at a lower voltage for a longer time, as this Lass5 was also a polyclonal antibody.

There are also a multitude of reasons as to why a change at the mRNA level would not be reflected at the protein level, such as protein degradation, rate of translation, and the marking of proteins to be degraded via post-translational modifications. However, a way to circumvent the last option would be for a protein to bind to a partner in order to decrease its chances of being degraded or destroyed.

Figure 9B shows the Duolink image for the CerS5 individual transfection condition. The blue DAPI staining in this image seems to be distributed a bit unevenly,

which may have been due to the fact that the DAPI staining was contained within the mounting medium and was not applied to the slides otherwise. There is very little green in that slide despite it have received the same COX4 antibody as the others. As with the CerS6 slide, this may have been a result of the fixative agent or simply the incorrect dilution was utilized. The CerS5 slide did show puncta, however, which indicates that cells overexpressing CerS5 may contain some endogenous CerS2 and those proteins were within range for the PLA probes. The puncta seem to be located along the juxtanuclear region, which would be appropriate for these ER-localized enzymes. The presence of endogenous CerS2 within CerS5-overexpressing cells is interesting especially because there was no indication of any CerS2 within CerS6-overexpressing cells, the isoform closest in identity to CerS5. Human error could have certainly contributed to this and this experiment would definitely merit from some repeat experiments, but if true, this is an interesting indication of the differences between CerS5 and CerS6. Both catalyze the same length ceramides, though some previous research has shown that CerS5 and CerS6 have different preferences toward saturated or unsaturated fatty acyl-CoA's (Mizutani et al., 2005). That seems to be the main difference as of late due to difficulties in distinguishing between CerS5 and CerS6 activity as they utilize the same acyl-CoA. However, Duolink PLA is limiting in that it does not necessarily show the presence of a protein, only whether that protein is within 40 nm of the other of interest and if the two interact.

Figure 9: Cells overexpressing CerS5 also express endogenous CerS2. (A) From this western blot run with the same Lass5 antibody used in immunofluorescence experiments, the darkest band is at the hCerS5 individual transfection condition. There is also a band in the hCerS2 transfection lane, which would mean that there is indeed endogenous CerS5 contained within CerS2-overexpressing cells at the protein level and enough of it to respond to the Lass5 antibody. The bands at the two co-transfection conditions almost appear the same, which may be due to the presence of endogenous CerS5 within CerS2-overexpressing cells responding to the antibody in either transfection, as previous research has shown that CerS2 can upregulate its enzymatic rate via dimerization. (B) The Duolink image of the CerS5 individual transfection shows puncta juxtanuclear to one of the cells, indicating that there may be endogenous CerS2 found within cells overexpressing CerS5.

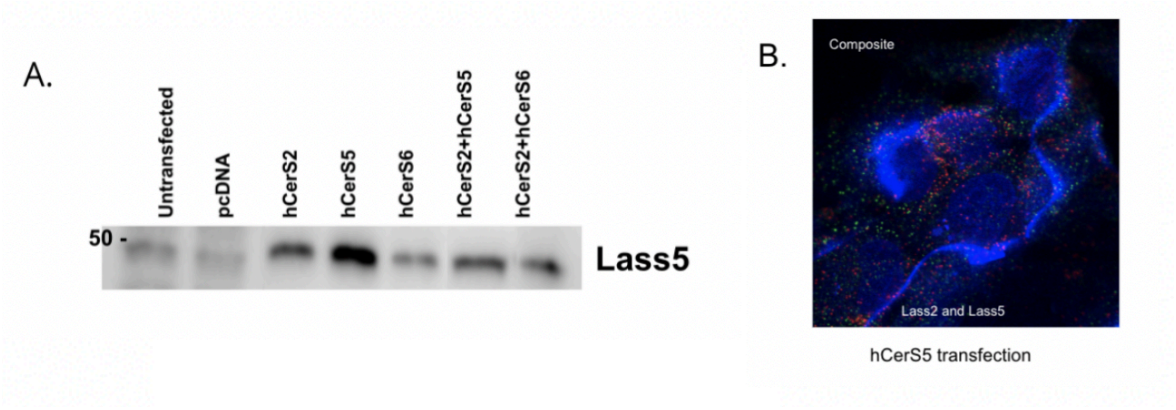

Figure 10A showed that the Lass2 antibody used was quite specific, as the only bands present are in transfection conditions that contained CerS2. Again, unlike what the mRNA had shown, the largest band is in the hCerS2 individual transfection, though the band in hCerS2+hCerS6 does seem to be larger than the one in hCerS2+hCerS5, which was shown in the mRNA. The band size in hCerS2 may be a result of, again, the changes at the mRNA level not translating to those at the protein level, or it may be due to post-translational modifications that occurred while the protein was being processed. Glycosylation and phosphorylation are the two main modifications that the CerS isoforms can undergo, and with the imaging showing that CerS2 may be localized to the Golgi, it would not be unreasonable to believe that the large CerS2 band may come from glycosylation of the protein. Regarding what was seen earlier with endogenous CerS2 within CerS5-overexpressing cells via the Duolink, it may not show on the western as a result of it being a transient interaction and too quick or too weak for the western blot to pick up.

The Duolink in Figure 10B shows some contrasting information to what had been seen previously regarding the presence of endogenous CerS5 within cells overexpressing CerS2 as there is no puncta present when CerS2 was subjected to Lass2 and Lass5. This may be a result of the initial CerS5/Lass5 western blot needing to be rerun or it could have resulted from the time that these cells were fixed for preparation. Both the western blot and Duolink are intended to illuminate as to what goes on at the protein level so this discrepancy is certainly one that would merit some additional testing though, again the Duolink PLA does not necessarily indicate presence of protein, just whether there is an

interaction between the two proteins of interest. Co-immunoprecipitation would be a tool of value to use at this point.

The Duolink with Lass2 and Lass6 does show some robust puncta juxtanuclear to the cells, which does correspond to what was seen with the CerS6/Lass6 western blot. All blots were run under the same conditions at the same time but again, the risk of human error is always present in such experiments. The western and the Duolink do coincide with their findings, which would make a strong argument for the presence of endogenous CerS6 within cells overexpressing CerS2, which again may come from the need to modulate pro- and anti-apoptotic lipids throughout the body.

Figure 10: Cells overexpressing CerS2 interact with CerS6 but may not with CerS5. (A) The Lass2 antibody was indeed specific to CerS2, possibly more so than Lass5 or Lass6 as it was a monoclonal antibody that could handle being run at a higher voltage. The largest band is present in the hCerS2 individual transfection rather than either of the co-transfections, which does not coincide with what was seen at the mRNA level. The band in hCerS2+hCerS6 does seem to be a little larger than that of hCerS2+hCerS5, which would coincide with what was seen at the mRNA level, but only marginally. (B) The Duolink for the CerS2 individual transfection is interesting because it clashes with one previous finding while strengthening another. There are no puncta present in the slide that received the Lass2 and Lass5 antibody, which would indicate a lack of interaction between CerS5 and CerS2 in these CerS2-overexpressing cells. However, there is puncta present when CerS2 receives Lass2 and Lass6, indicating that there is the presence of endogenous CerS6 within the cells and the two isoforms are close enough to create puncta via the PLA probes and potentially dimerize.

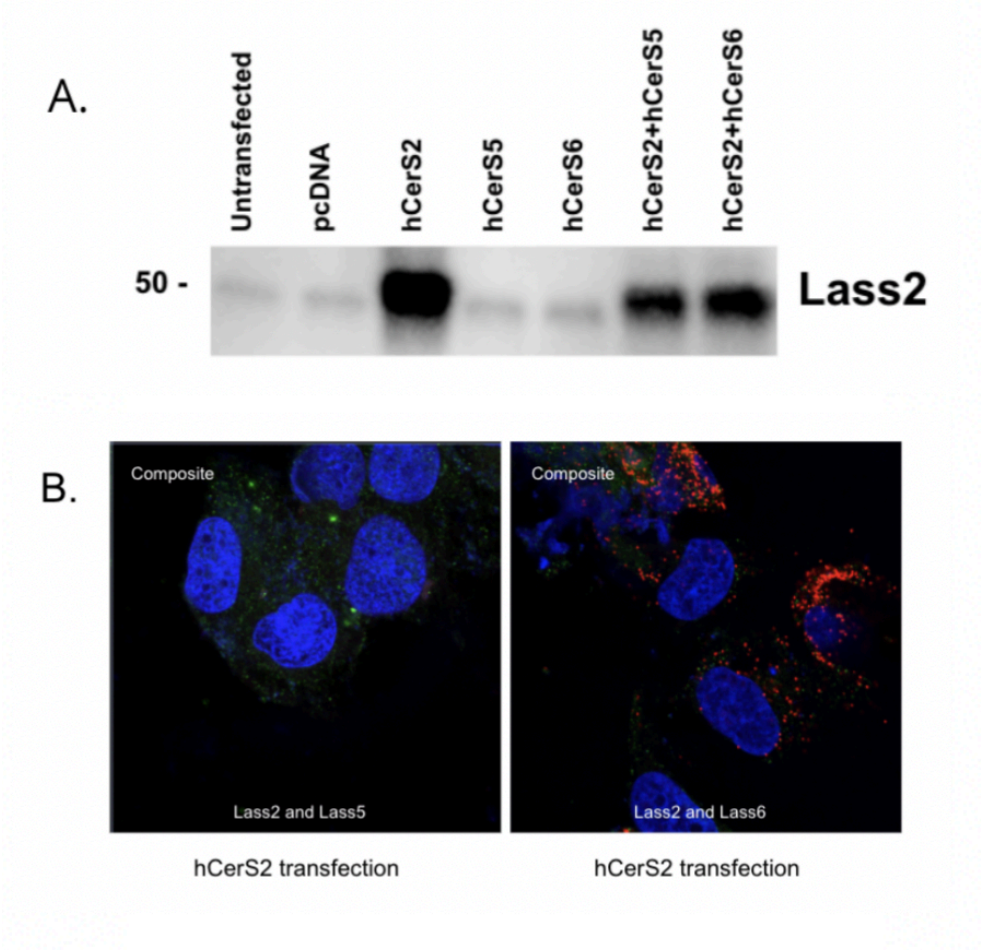
A.
Untransfected
pcDNA
hCerS2
hCerS5
hCerS6
hCerS2+hCerS5
hCerS2+hCerS6
50 -
Lass2
B.
Composite
Lass2 and Lass5
Composite
Lass2 and Lass6
hCerS2 transfection
hCerS2 transfection

Discussion

The comprehension of the molecular and regulatory mechanisms of ceramide synthases is a crucial step to take in order to better understand an incredibly important molecule within our bodies. As mentioned previously, ceramides are the backbone of bioactive sphingolipids that are interwoven with a number of processes at the cellular level. Ceramide and sphingolipid metabolite dysregulation can lead to issues with cellular apoptosis as well as cell proliferation; some common examples include Alzheimer's, Huntington's disease, cardiovascular disease, and many human cancers, all of which have been noted to involve some aspect of ER stress. Ceramides have also been observed to regulate key intracellular effectors that will actually mediate the action of those same ceramides regarding apoptotic instructions (Pettus et al., 2002).

Due to the range in chain lengths of the fatty acids produced, ceramide synthases are considered a family of molecules rather than simply a single molecule. Ceramide synthases have also been categorized into six different isoforms, with the majority of them being relatively similar to one another, aside from CerS1 which has been well documented to be both structurally and functionally distinct from its sisters (Sridevi et al., 2010; Min et al., 2007). Of the six, CerS2 and CerS5 are considered the isoforms with the best understood regulatory mechanisms while CerS6 remains mostly a mystery. CerS5 and CerS6 actually share a high level of identity and similarity and CerS6 seems to be an ER-residing protein like CerS2. However, CerS5 and CerS6 have different distributions throughout the body and seem to have different substrate preferences regarding unsaturated

or saturated fatty acyl-CoA's (Mizutani et al., 2005), though both can and do utilize palmitoyl-CoA to produce C_{16}-ceramides as they share substrate specificity levels (Novgorodov et al., 2010).

This project was focused on CerS2, CerS5, and CerS6 with a primary aim of determining whether co-overexpression affected localization and/or enzyme expression levels as measured by using immunofluorescence. Past research has shown that ceramide synthase activity was augmented in microsomes, with ceramidase activity present in mitochondrial fractions and mitochondria-associated membranes (Mullen et al., 2013). Novgorodoc and Gudz, in 2009, found that mitochondrial enzymes showed twice as much CerS activity as compared to those from the ER. CerS6 expression, interestingly, had been observed to have no effect on mitochondrial ceramide localization or mitophagy, with the researchers believing that subcellular localization of ceramides, rather than their acyl chain lengths, played a large role in determining their biological functions (Jiang and Ogretman, 2013).

Sphingomyelinases contribute to the second known mechanism of producing ceramides from sphingolipids (thought of as the recycling/reverse or the acyl-CoA-independent pathway), though its significance regarding actual ceramide production is still unclear as the primary mechanism is regarded as the *de novo* process using ceramide synthases. CerS2 and CerS5 have both been found to localize to the ER (Mizutani et al., 2005; Laviad et al., 2007), though it is of worth to note that Wenger et al., in 2016, were unclear regarding if discrete localizations of each isoform may be due to unspecific antibodies, artifacts, or cellular modifications. Wenger et al. had seen that there were

differences in localization of CerS5 and CerS6, possibly due to cellular remodeling or antibody cross-reactivity.

Via qPCR in 2012, Laviad et al. found that, while CerS2 mRNA has the highest levels and the broadest tissue distribution of the isoforms, it also had the lowest *in vitro* enzymatic activity. In mammals, CerS2 activity is the most upregulated (to the point where Wenger et al. postulated that it may even act as a housekeeping gene in 2016) and requires both more time and higher protein concentration in order to match the same enzymatic levels as the other isoforms (Zelnik et al., 2019). That lack of enzymatic activity was the basis for Zelnik et al.'s 2019 study on whether CerS2 dimerizes in order to augment its activity levels. Mesicek et al., in 2010, had also postulated that there may be a physical interaction between the CerS isoforms. In 2012, Laviad et al. looked into further qualifying how CerS activity is regulated and found that, not only can CerS form dimers and co-immunoprecipitate together, but CerS2 activity was enhanced upon co-overexpression with both CerS5 and CerS6. The researchers had also found that, in a heterodimer of CerS2 and CerS5, the activity of CerS2 depended upon the catalytic activity of CerS5.

Generally, an mRNA increase would indicate an increase in protein levels, though the comprehension of CerS expression at the mRNA level is still one to be furthered as it is considerably still uncharacterized. RT qPCR primers also do have different binding affinities, which may have affected the overall read of each gene's expression level. Regarding the large band in the Lass2 blot (Figure 10A) and any post-translational modifications that the CerS may undergo, glycosylation has not been deemed for their enzymatic activities (Novgorodov and Gudz, 2009). CerS2, CerS5, and CerS6 are all N-

glycosylated (Mizutani et al., 2005). CerS2 through CerS6 are also phosphorylated at the C-terminal, with CerS2 activity being heavily reliant upon this specific post-translational modification while the activities of CerS5 and CerS6 are only mildly increased (Sassa et al., 2016). Phosphorylation of ceramide synthases seems to be a more likely occurrence for these enzymes, though Sassa et al. has seen that hyperactivation of the CerS species by phosphorylation may worsen pathological conditions if sphingolipid species accumulate. Regarding this project and any future endeavors, it absolutely would have been of worth to test for glycosylation versus phosphorylation of these species by utilizing a phosphorylated version of these antibodies, though none seem to be commercially available at this time. Another option within that same vein would have been to subject the samples to enzymatic deglycosylation as it has been seen that CerS5 activity increases upon deglycosylation *in vitro* (Wegner et al., 2016). Glycosylation could have also played a part in why the CerS2 individual transfection condition Duolink did not show any puncta when probed with Lass2 and Lass5 (Figure 10B).

In HeLa cells in 2012, Sassa et al. found that the knockdown of the CERS2 gene caused a downstream decrease in C_{24}-ceramide while also creating a compensatory increase in C_{16}-ceramide; said compensation may be the basis for the presence of endogenous CerS6 (and possibly CerS5) within cells overexpressing CerS2 at the protein level. Long-chain (C_{16}) and very long-chain (C_{24}) sphingolipids are the two most predominant forms found in most mammalian tissues and their functions range widely enough to the point where dysfunction or dysregulation could be major pathological issues. LC and VLC sphingolipids are produced mainly by CerS6 or CerS5 and CerS2,

respectively, and have been found to co-exist in order to maintain the proper balance between pro- and anti-apoptotic behavior in the body.

Between the qPCR's, the western blots, and the Duolink images, it can be said that the transfections, primers, and antibodies all work at both the mRNA and protein level, though there was not as much visible change with the protein as was with the mRNA. To further confirm transfection identities for a repeat of this project, a lipidomic study could have been done for the samples, which was ultimately unable to be included in this project. Another experiment that would have been of worth doing and has been mentioned previously in this thesis would have been co-immunoprecipitation of CerS2 with either CerS5 or CerS6 in order to further validate changes seen at the protein level with co-overexpression. SDS-PAGE and western blotting has confirmed that CerS2 immunoprecipitates with CerS6 and CerS5 can immunoprecipitate with both CerS2 and CerS6 (Laviad et al., 2012; Mesciek et al, 2010).

Via immunofluorescence, it was shown that CerS2 does localize to the cell differently compared to that of CerS5 and CerS6 in that CerS2 is brightest immediately juxtanuclear around the ER as well was in the Golgi. CerS1, the most structurally unique isoform, has been able to translocate to the Golgi under certain stressors or chemotherapeutic drugs, though that same behavior was not seen in CerS5 when tested (Min et al., 2007; Sridevi et al., 2010). All three of the CerS of interest to this project have previously been shown to localize to the ER, which was reinforced with this project via immunofluorescence experiments, though CerS5 and CerS6 both appear to also localize to the mitochondria.

Literature Cited

1. Alayoubi, Abdulfatah M., et al. “Systemic Ceramide Accumulation Leads to Severe and Varied Pathological Consequences.” *EMBO Molecular Medicine*, vol. 5, no. 6, 2013, pp. 827–842., doi:10.1002/emmm.201202301.
2. Alam, Muhammad S. “Proximity Ligation Assay (PLA).” *Current Protocols in Immunology*, vol. 123, no. 1, 2018, doi:10.1002/cpim.58.
3. Bio-Rad. “Introduction to Western Blotting: Bio-Rad.” Bio, www.bio-rad-antibodies.com/western-blotting-immunoblotting-introduction.html.
4. Gault, Christopher R., et al. “An Overview of Sphingolipid Metabolism: From Synthesis to Breakdown.” *Advances in Experimental Medicine and Biology Sphingolipids as Signaling and Regulatory Molecules*, 1 Apr. 2011, pp. 1–23., doi:10.1007/978-1-4419-6741-1_1.
5. Hannun, Yusuf A., and Chiara Luberto. “Ceramide in the Eukaryotic Stress Response.” Trends in Cell Biology, vol. 10, no. 2, 2000, pp. 73–80., doi:10.1016/s0962-8924(99)01694-3.
6. Jiang, Wenhui, and Besim Ogretmen. “Ceramide Stress in Survival versus Lethal Autophagy Paradox.” Autophagy, vol. 9, no. 2, 2013, pp. 258–259., doi:10.4161/auto.22739.
7. Lavieu, Gregory, et al. “Is Autophagy the Key Mechanism by Which the Sphingolipid Rheostat Controls the Cell Fate Decision?” *Autophagy*, vol. 3, no. 1, 2007, pp. 45–47., doi:10.4161/auto.3416.

8. Laviad, Elad L., et al. “Characterization of Ceramide Synthase 2.” Journal of Biological Chemistry, vol. 283, no. 9, 2007, pp. 5677–5684., doi:10.1074/jbc.m707386200.
9. Laviad, Elad L., et al. “Modulation of Ceramide Synthase Activity via Dimerization.” Journal of Biological Chemistry, vol. 287, no. 25, 2012, pp. 21025–21033., doi:10.1074/jbc.m112.363580.
10. Levy, Michal, and Anthony H. Futerman. “Mammalian Ceramide Synthases.” *IUBMB Life*, 1 May 2011, doi:10.1002/iub.319.
11. Mesicek, Judith, et al. “Ceramide Synthases 2, 5, and 6 Confer Distinct Roles in Radiation-Induced Apoptosis in HeLa Cells.” Cellular Signalling, vol. 22, no. 9, 2010, pp. 1300–1307., doi:10.1016/j.cellsig.2010.04.006.
12. Min, J., et al. “(Dihydro)Ceramide Synthase 1 Regulated Sensitivity to Cisplatin Is Associated with the Activation of p38 Mitogen-Activated Protein Kinase and Is Abrogated by Sphingosine Kinase 1.” Molecular Cancer Research, vol. 5, no. 8, Jan. 2007, pp. 801–812., doi:10.1158/1541-7786.mcr-07-0100.
13. Mizutani, Yukiko, et al. “Mammalian Lass6 and Its Related Family Members Regulate Synthesis of Specific Ceramides.” Biochemical Journal, vol. 390, no. 1, Sept. 2005, pp. 263–271., doi:10.1042/bj20050291.
14. Mullen, Thomas D., et al. “Ceramide Synthases at the Centre of Sphingolipid Metabolism and Biology.” Biochemical Journal, vol. 441, no. 3, 2012, pp. 789–802., doi:10.1042/bj20111626.

15. Novgorodov, Sergei A, and Tatyana I Gudz. “Ceramide and Mitochondria in Ischemia/Reperfusion.” Journal of Cardiovascular Pharmacology, vol. 53, no. 3, 2009, pp. 198–208., doi:10.1097/fjc.0b013e31819b52d5.

16. Novgorodov, Sergei A., et al. “Developmentally Regulated Ceramide Synthase 6 Increases Mitochondrial Ca2 Loading Capacity and Promotes Apoptosis.” Journal of Biological Chemistry, vol. 286, no. 6, Oct. 2010, pp. 4644–4658., doi:10.1074/jbc.m110.164392.

17. Pettus, Benjamin J., et al. “Ceramide in Apoptosis: an Overview and Current Perspectives.” Biochimica Et Biophysica Acta (BBA) - Molecular and Cell Biology of Lipids, vol. 1585, no. 2-3, 2002, pp. 114–125., doi:10.1016/s1388-1981(02)00331-1.

18. Pewzner-Jung, Yael, et al. “When Do Lasses (Longevity Assurance Genes) Become CerS (Ceramide Synthases)?” *Journal of Biological Chemistry*, vol. 281, no. 35, 2006, pp. 25001–25005., doi:10.1074/jbc.r600010200.

19. Ponnusamy, Suriyan, et al. “Sphingolipids and Cancer: Ceramide and Sphingosine-1-Phosphate in the Regulation of Cell Death and Drug Resistance.” *Future Oncology*, vol. 6, no. 10, 2010, pp. 1603–1624., doi:10.2217/fon.10.116.

20. Russo, Sarah Brice, et al. “Ceramide Synthase 5 Mediates Lipid-Induced Autophagy and Hypertrophy in Cardiomyocytes.” Journal of Clinical Investigation, vol. 122, no. 11, Jan. 2012, pp. 3919–3930., doi:10.1172/jci63888.

21. Sassa, Takayuki, et al. “A Shift in Sphingolipid Composition from C24 to C16 Increases Susceptibility to Apoptosis in HeLa Cells.” Biochimica Et Biophysica

Acta (BBA) - Molecular and Cell Biology of Lipids, vol. 1821, no. 7, 2012, pp. 1031–1037., doi:10.1016/j.bbalip.2012.04.008.

22. Sassa, Takayuki, et al. “Enzyme Activities of the Ceramide Synthases CERS2–6 Are Regulated by Phosphorylation in the C-Terminal Region.” Journal of Biological Chemistry, vol. 291, no. 14, 2016, pp. 7477–7487., doi:10.1074/jbc.m115.695858.
23. Senkal, Can E., et al. “Alteration of Ceramide Synthase 6/C16-Ceramide Induces Activating Transcription Factor 6-Mediated Endoplasmic Reticulum (ER) Stress and Apoptosis via Perturbation of Cellular Ca2 and ER/Golgi Membrane Network.” Journal of Biological Chemistry, vol. 286, no. 49, 2011, pp. 42446–42458., doi:10.1074/jbc.m11
24. Senkal, Can E., et al. “Antiapoptotic Roles of Ceramide-Synthase-6-Generated C16-Ceramide via selective Regulation of the ATF6/CHOP Arm of ER-Stress-Response Pathways.” The FASEB Journal, vol. 24, no. 1, 2010, pp. 296–308., doi:10.1096/fj.09-135087.1.287383.
25. Sridevi, Priya, et al. “Stress-Induced ER to Golgi Translocation of Ceramide Synthase 1 Is Dependent on Proteasomal Processing.” Experimental Cell Research, vol. 316, no. 1, 2010, pp. 78–91., doi:10.1016/j.yexcr.2009.09.027.
26. Vogel, Christine, and Edward M. Marcotte. “Insights into the Regulation of Protein Abundance from Proteomic and Transcriptomic Analyses.” *Nature Reviews Genetics*, vol. 13, no. 4, 2012, pp. 227–232., doi:10.1038/nrg3185.

27. Wegner, Marthe-Susanna, et al. “The Enigma of Ceramide Synthase Regulation in Mammalian Cells.” Progress in Lipid Research, vol. 63, 2016, pp. 93–119., doi:10.1016/j.plipres.2016.03.006.

28. Wojewodka, Gabriella, et al. “Ceramide in Cystic Fibrosis: A Potential New Target for Therapeutic Intervention.” *Journal of Lipids*, vol. 2011, Jan. 2011, pp. 1–13., doi:10.1155/2011/674968.

29. Zelnik I.D., Rozman B., Rosenfeld-Gur E., Ben-Dor S., Futerman A.H. (2019) A Stroll Down the CerS2 Lane. In: Stiban J. (eds) Bioactive Ceramides in Health and Disease. Advances in Experimental Medicine and Biology, vol 1159. Springer, Cham., doi:10.1007/978-3-030-21162-2_4

30. Zhang, Jitao David, et al. “DdCt Method for QRT-PCR Data Analysis.” Bioconductor, 27 Apr. 2020, www.bioconductor.org/packages/devel/bioc/vignettes/ddCt/inst/doc/rtPCR.pdf.

31. Zheng, Wenjing, et al. “Ceramides and Other Bioactive Sphingolipid Backbones in Health and Disease: Lipidomic Analysis, Metabolism and Roles in Membrane Structure, Dynamics, Signaling and Autophagy.” *Biochimica Et Biophysica Acta (BBA) - Biomembranes*, vol. 1758, no. 12, 2006, pp. 1864–1884., doi:10.1016/j.bbamem.2006.08.009.

VITA

Dorothy Yen was born in Washington, DC on August 2nd, 1994. She lived in Silver Spring, Maryland until she was twelve when her family moved to Northern Virginia. Her parents still live there today. She went to Virginia Commonwealth University in Richmond, VA for her degrees in Foreign Language with a Concentration in French as well as Biology. She also obtained a minor in Chemistry following the pre-med track. Two years after her graduation in 2016, she enrolled in the Pre-medical Graduate Certificate Program at Virginia Commonwealth University in order to better her application for medical school. It was during this time that she began working in the Cowart Lab as a lab assistant. Upon graduation, she will be moving to Meridian, Idaho in order to pursue medicine at the Idaho College of Osteopathic Medicine, Class of 2024. She hopes to become a general surgeon, possibly with a subspecialty in Critical Care.